Rev. Adv. Mater. Sci. 39 (2014) 1-8

OPTIMIZED APPROACH FOR SYNTHESIS OF NANOTWINNED COPPER WITH ENHANCED HARDNESS

V.G. Konakov[1,2,3,4], O. Yu. Kurapova[1,2,4], N.N. Novik[1,2,4], S.N. Golubev[4], A.V. Osipov[3,5], A.S. Graschenko[3], A. P. Zhilyaev[1,6], S. N. Sergeev[6] and I.Yu. Archakov[1,2,3,4]

[1]Research Laboratory for Mechanics of New Nanomaterials, St. Petersburg State Polytechnical University, Polytechnicheskaya 29, St.Petersburg 195251, Russia
[2]Insitute of Chemistry and Department of Mathematics and Mechanics, St. Petersburg State University, Universitetskii pr. 26, Petrodvorets, St. Petersburg, 198504, Russia
[3]Institute of Problems of Mechanical Engineering, Russian Academy of Sciences, Bolshoy pr. 61, V.O., St. Petersburg 199178, Russia
[4]Scientific and Technical Center "Glass and Ceramics", 20 lit. A, 9 linia V.O., St.Petersburg, 199004, Russia
[5]St. Petersburg Academic University, Khlopina 8/3, St. Petersburg, 194021, Russia
[6]Institute for Metals Superplasticity Problems, Khalturina 39, Ufa 450001, Russia

Received: October 23, 2014

Abstract. Optimized approach for nanotwinned copper synthesis via electrodeposition technique is described. SEM, EBSD, XRD, and Nanoindentation tests of the synthesized layers were performed. The results of the tests demonstrate good surface quality and improved hardness.

1. INTRODUCTION

Nanotwinned metals (NTM) are considered as perspective materials providing the opportunity to achieve high strength properties [1,2] along with some other positive modifications like electroconductivity improvement [3]. Basing on theoretical considerations, authors of [1,2] are discussing possible advantages of NTM over ultrafine-grained (UG) and nanocrystalline (NC) materials due to the fact that UG and NC materials are strengthened through traditional grain boundaries which are incoherent and defective [4]. Strengthening of NTM through coherent twin boundaries [1,2] provides higher mechanical properties.

NTMs are generally manufactured by magnetron sputtering, see e.g. [2]. However, the possibility to synthesize nanotwinned copper by electrodeposition (in its pulsed or direct-current version) reported in the works by L. Lu et al. [3,5-8] seems to be much time/cost-effective approach. In addition, thicker deposition layers can be produced by electrodeposition technique (tens or even hundreds of microns).

Above mentioned papers [3,5-8] prove the unique properties of nanotwinned copper. Ref. [3] compares the true stress of nanotwinned copper with the data obtained for nanocrystalline and coarse-grained Cu. As could be seen from [3], the true stress of nanotwinned copper is much higher than that for coarse-grained Cu. In spite of the fact that the exact data on nanocrystalline copper true stress are not presented for the wide true strain range, the behavior of the curve gives an opportunity to assume that true stress of nanotwinned copper is also higher than that for nanocrystalline one. As for the values of the electrical resistivity, the analysis of the resistivity vs

Corresponding author: V.G. Konakov, e-mail: glasscer@yandex.ru

© 2014 Advanced Study Center Co. Ltd.

temperature dependencies demonstrates the significant advantage of nanotwinned Cu. The detailed analysis of tensile behavior of nanotwinned Cu and its microstructure is also given in [7], the conclusions on the inhomogeneity of the plastic deformation of columnar-grained nanotwinned copper and the strong effect of the grain size on the ductility and work hardening capacity are formulated.

Ref. [5] discusses the effect of mean twin thickness on the yield strength and strain hardening coefficient of nanotwinned copper. The authors state that the strength of the studied samples is increasing with the decrease in the twin thickness and consider the twin thickness of 15 nm as being a condition of the maximal strength value.

Paper [6] reports the effect of the cold rolling performed at room temperature and liquid nitrogen temperature on the mechanical properties of nanotwinned copper samples and their deformation mechanisms. The increase in the hardness of the nanotwinned copper samples rolled at room temperature is evident (from 2.5 to 3.0 GPa), while low temperature rolling gives rise to some slight hardness decrease (from 2.33 to 2.21 GPa). The authors of the paper consider these variations as proceeding due to changes in the nanotwinnned state of the material.

The results of nanoindentation tests of nanotwinned Cu are discussed by Choi et al. [9]. The paper compares the results obtained for nanotwinned and single crystal copper samples, the conclusion on the different behavior is done.

As seen from the above consideration, the possibility to obtain nanotwinned copper possessing elevated mechanical properties is of high interest. The method of electrodeposition appears to be a promising technique for nanotwinned materials manufacturing. However, a careful optimization of different parameters (the composition of the solution, the deposition cell geometry, current density, time of the deposition etc.) is required. Thus, the task of the work is the optimization of the electrodeposition approach in order to couple the method time/cost effectiveness with the highest yield in the deposited layer thickness. The present paper describes the possible trend of such optimization, the data of SEM, ESBD, XRD, and Nanoindentation tests are discussed.

2. EXPERIMENTAL

Nanotwinned copper films were deposited from aqueous or ethanol-aqueous solution of copper sulphate ($CuSO_4$) using electrodeposition technique. The deposition was performed in both direct current and pulse versions of the technique. In order to provide better surface quality along with the high deposition rate, a number of approaches were tested. They differ in the solution compositions, the deposition cell geometry (electrode shapes, distances between the electrodes, anode-to-cathode surface ratio, etc.). All experiments include copper (>99.99 at.%) anode and stainless steel (X10CrNi18-8, i.e. SAE grade 301) was the cathode material.

2.1. Preparation of the initial solutions

Solution #1. 1 M aqueous copper sulphate solution was prepared by crystal hydrate $CuSO_4 \cdot 6H_2O$ (99.99%) dissolution in distilled water at 25 °C. The solution was then acidified by H_2SO_4 up to pH=1.

Solution #2. 1 M aqueous copper sulphate solution was prepared by crystal hydrate $CuSO_4 \cdot 6H_2O$ (99.99%) dissolution in distilled water at 25 °C. Then the ethanol was added up to its 75 mL/L content. The solution was then acidified by H_2SO_4 up to pH=1.

Solution #3. 1 M aqueous copper sulphate solution was prepared by crystal hydrate $CuSO_4 \cdot 6H_2O$ (99.99%) dissolution in distilled water at 25 °C. Then the ethanol was added up to its 37.5 mL/L content. The solution was then acidified by H_2SO_4 up to pH=1.

2.2. Deposition cell geometry

Cell #1. Glass cylinder (∅ 60 mm). The copper rod (anode) was placed in the center of the cylinder, while the stainless steel cylinder (foil) was adjusted to the cell wall. The anode-to-cathode surface ratio here was 1/30, according to [3], such a geometry gives an opportunity to obtain uniform and dense deposition layer on the whole cathode surface. Electrodeposition was performed at 0.5 A direct current (DC Power Supply HY3665D) maintaining pH=1, the duration of the process was 1 hour.

Solutions ## 1-3 were used to produce Samples NN 1-3, respectively. Resulting samples were washed in the distilled water, dried by ethanol, and then copper foil was partly removed from the stainless steel substrate.

Cell #2. The electrodes used here were coplanar plates; the ratio of anode-to-cathode surface ratio was inverted, in this version the anode surface was 16 times higher than the cathode one (25x20x5 mm stainless steel cathode and 100x80x5 mm copper anode). The distance between the electrodes was 30 mm. The deposition conditions were the same as described for Cell #1, Solution #3 was used to manufacture Sample #4. This sample was washed,

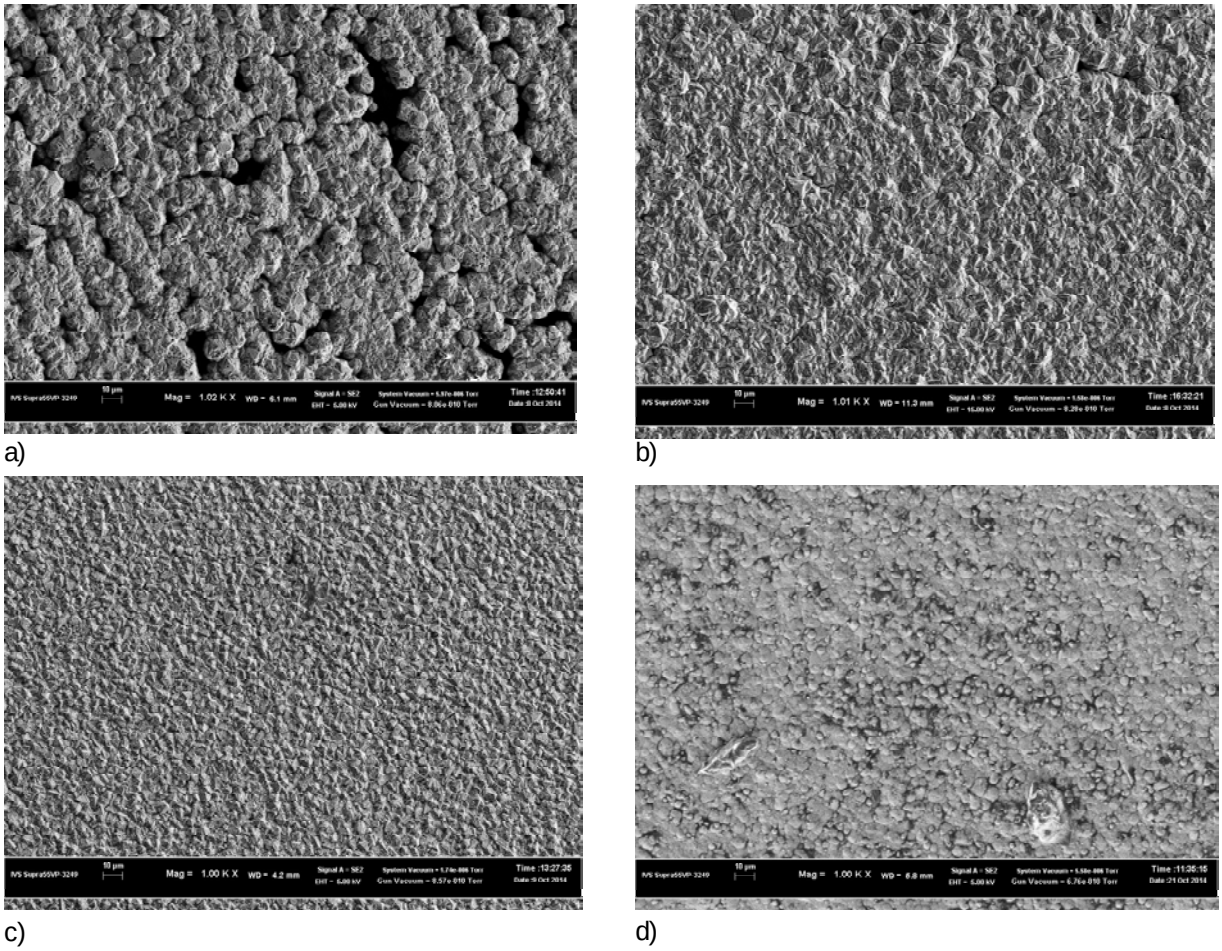

a) b) c) d)

Fig. 1. Copper film surface, a, b, c, d – Samples NN 1, 2, 3, 4, respectively.

dried and partly removed from the substrate according to the procedure reported above.

Cell #3. The geometry of the cell was the same as for Cell #2. However, the deposition was performed in the pulse regime. The pulse on-time was 0.02 s and the off-time was 2 s. Since the copper film growth rate from Solution #3 was the highest, this solution was used for pulse experiments. To avoid solution depletion in copper, we have decreased the effective peak current down to 0.2 mA; in turn, the deposition duration was increased up to 24 hours. As a result, Sample # 5 was produced, it was also washed in the distilled water and dried. However, the thickness of the copper film was too small to remove it from the substrate foil.

2.3. Testing approaches and equipment

The microstructure of all samples was studied using scanning electron microscopy (SEM, Zeiss Supra V-55), microphotos of both outer and internal (adjacent to stainless steel foil) surfaces were collected. EBSD approach was used to prove the twinned structure. The EBSD analysis was performed using a TESCAN MIRA 3LMH FEG scanning electron microscope equipped with an EBSD analyzer “CHANNEL 5“ and a rectangular grid with scan step of 50 nm was used. The acquired data were subjected to standard clean-up procedures involving a grain tolerance angle of 5° and a minimum grain size of three pixels. The grain sizes were measured using the linear intercept as the distances between high-angle boundaries with misorientations above 15°. X-ray diffraction (XRD) Shimadzu XRD-6000, Cu K_{α} with λ= 1.54 Å, analysis was performed at room temperature (RT). Nanoindentation tests were carried out using NanoTest (Micro Materials Co.) equipment.

3. RESULTS AND DISCUSSION

3.1. SEM study

Since the thickness of the coating obtained using pulse version of the electrodeposition (Cell #3, Sample 5) was insufficient, the results of SEM study are presented for Samples NN 1-4. Fig. 1 illustrates

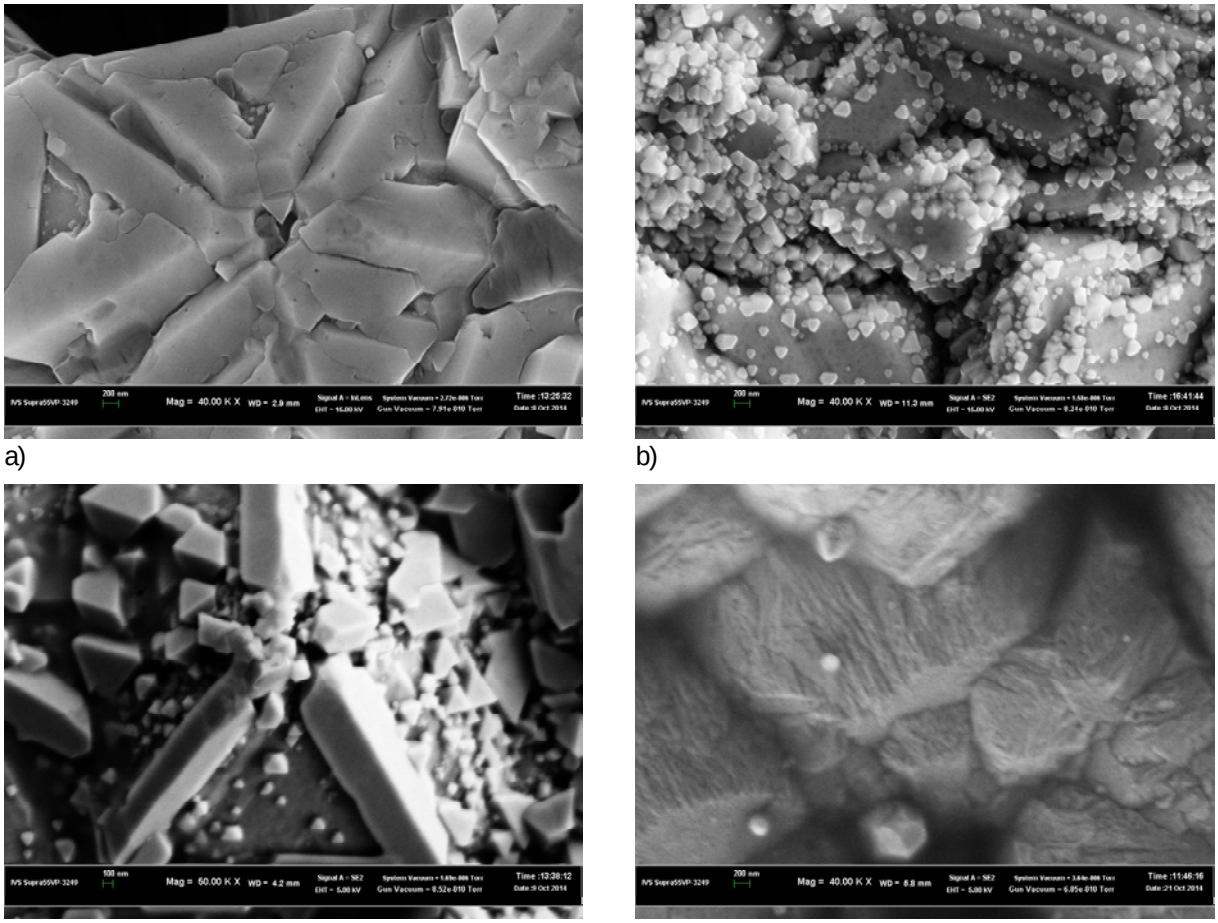

a) b) c) d)

Fig. 2. Microstructure of copper films, a, b, c, d – Samples NN 1, 2, 3, 4, respectively.

the general view of the surface. As seen from the microphotos, the surface of the layer obtained using aqueous solution (Fig. 1a) is rough, in addition, it is not compact enough. Some breaks are clearly seen here, their surface is fairly high. Ethanol addition (Fig. 1b) leads to more uniform and smooth surface, however, the surface is still rough. The use of Solution #3 provides the best results (Sample #3, Fig. 1c): the smooth and compact surface film was coupled with the high growth rate of 340 μm per hour. For this reason, this solution was used in Cell #2 with the inverted anode-to-cathode surface ratio, see Fig. 1d. As seen from this figure, Sample 4 possesses the highest surface quality. This statement can be proved by the analysis of Fig. 2.

These images demonstrate the typical microstructure of Samples NN1-4 surface. As can be seen from Figs. 2a-2c, the copper film growth in Cell#1 is not columnar nor epitaxial, polycrystals oriented on the edges and planes of octahedrons or triangular prisms are present. On the contrary, Sample 4 demonstrates smooth growth, Fig. 2d. As seen from Fig. 3, this Sample (Sample 4) is the only one characterized by nanosized crystallites.

So, the analysis of Figs. 1-3 prove that Cell#2 deposition conditions provides highly uniform nanosized films that can be produced with acceptable growth rate.

3.2. EBSD Results

Figs. 4 and 5 depicts EBSD data for electrodeposited copper (Sample 4). Fig. 4a corresponds to raw inverse pole figure (IPF) map acquired from the surface without any polishing. Selected area indicated by white rectangle in Fig. 4a with higher confidence index was cleaned up; the data obtained for this region are shown in Fig. 4b. Black lines in the map delineate twins. Fraction of twin boundaries is about 50% for this selected area. Discrete pole figure are shown in Fig. 4c. No specific orientations can be found. Microstructure of electrodeposited copper (Sample 4) possesses rather random texture, this fact is in agreement with XRD data (see Section

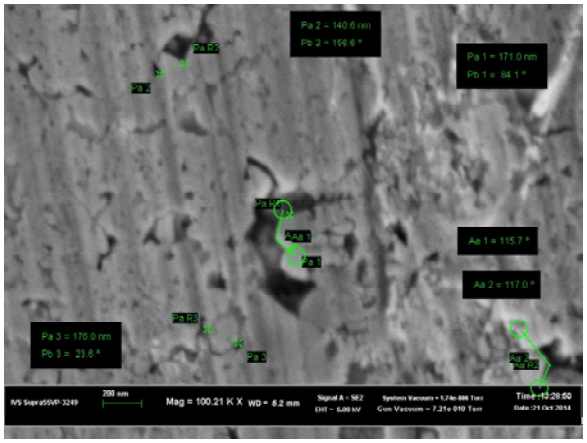

Fig. 3. Characterization of nanosized objects of Sample 4.

3.3. and Fig. 6). Grain boundary misorientation has a peak at 60° (Fig. 5) which corresponds to Σ3 boundaries. Total number fraction of twins is more than 50 percent.

3.3. XRD characterization

Fig. 6 depicts XRD patterns of Sample #4 (outer, 4a and inner 4b surfaces) compared with similar data obtained for Samples #1 (4c, outer surface) and #3 (4d, outer surface).

The analysis of the XRD patterns presented in Fig. 6 indicates that all outer surfaces (Figs. 6a, 6c, and 6d) patterns are quite similar. The comparison of Figs.6a and 6b gives an opportunity to conclude that the peaks corresponding to inner surfaces are slightly broadened, this is possibly due to smaller crystallites. Indeed, average crystallite sizes estimated using Sherrer's formula are 110 and 180 nm for inner and outer surface, respectively. Note, that this evaluation is in a good agreement with the data presented in Fig. 3; proving the nanosized structure of the copper film.

3.3. Nanoindentation tests

Nanoindentation tests and the computation of the mechanical properties were performed at 5, 10, 15, and 20 mN maximal loadings. The diamond Berkovitch indentor was used; loading/unloading rate was kept constant, it was 0.5 mN/s. The time between two experimental point on the curves is about 0.05 s. Fig. 7 demonstrates typical dependence of the force applied to the indentor on the depths of its

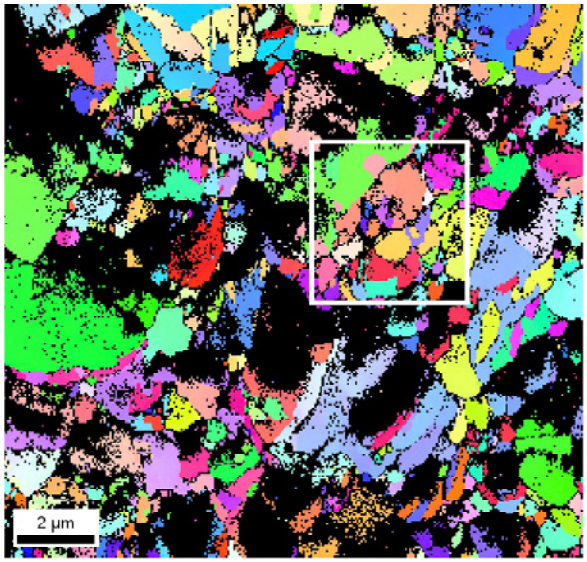

a)

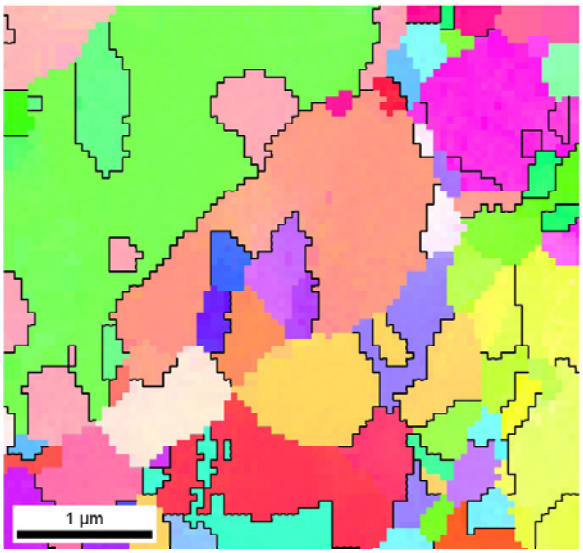

b)

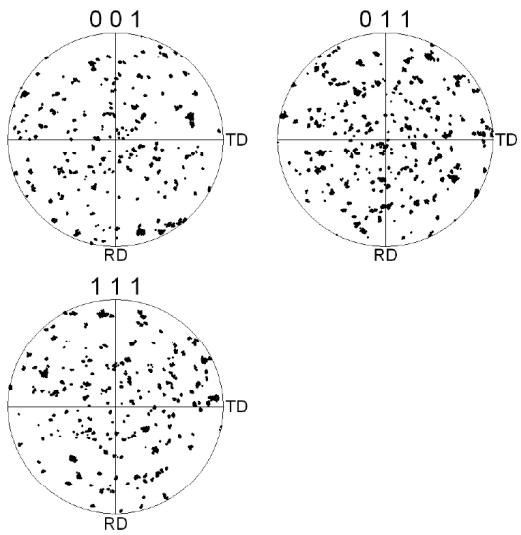

c)

Fig. 4. EBSD data for electrodeposited copper (Sample 4): (a) raw inverse pole figure (IPF) map; (b) IPF map of selected area indicated by white rectangle in (a); and (c) discrete pole figures.

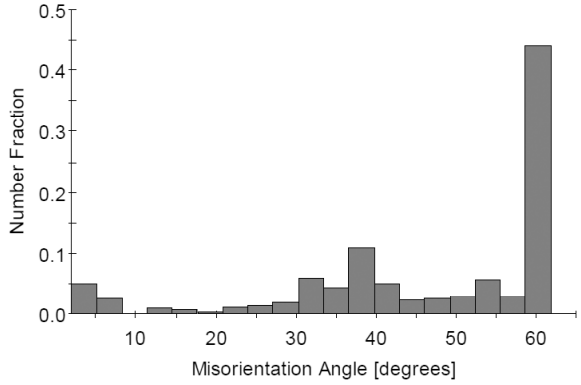

Fig. 5. Misorientation distribution for electrodeposited copper (Sample 4). Peak at 60° corresponds to twin boundaries.

penetration into the sample (*h*) for copper film (Sample 4) at maximal loadings of 10 и 20 mN.

As seen from Fig. 7, the deformation jumps appear on the curve at loadings over 8 mN. Possibly, it is due to the dislocation absorption in the deformation zone. On the other hand, similar plastic flow is sometimes associated with the dynamic deformation aging due to the interaction of the dislocations with the impurity atoms [10,11]. For 25% of nanoindentation tests the deformation jumps were registered at loadings lower than 10 mN (Fig. 8); this fact can be the reason of ≈ 45% decrease in hardness and ≈ 17% decrease in elastic modulus.

Hardness and elastic modulus were calculated using Oliver-Pharr approach, see, e.g. [12]. The dependence of average hardness values on the indentation depth is shown in Fig. 9, regarding for this data, the average hardness on the indentation depth less than 500 nm is 2.4 GPa. It decreases down to 1.5 GPa (37%) at the indentation depth of 800 nm.

Young's modulus vs indentation depth curves are demonstrated in Fig. 10. As seen from the figure, the Young's modulus decreases from 48 to 23 GPa with the increase in the nanoindentation depth. So, the Young's modulus value can be evaluated as 60 GPa.

The average elastic modulus calculated from Hertz curve can be estimated as 102 GPa [12]. Note that this approach bases on the analysis of the initial loading step when the deformation is elastic only. Since the initial step of nanoindentation with a high probability proceeds in a zone free of dislocations and far from grain boundaries, the above value can be treated as monocrystal characteristic.

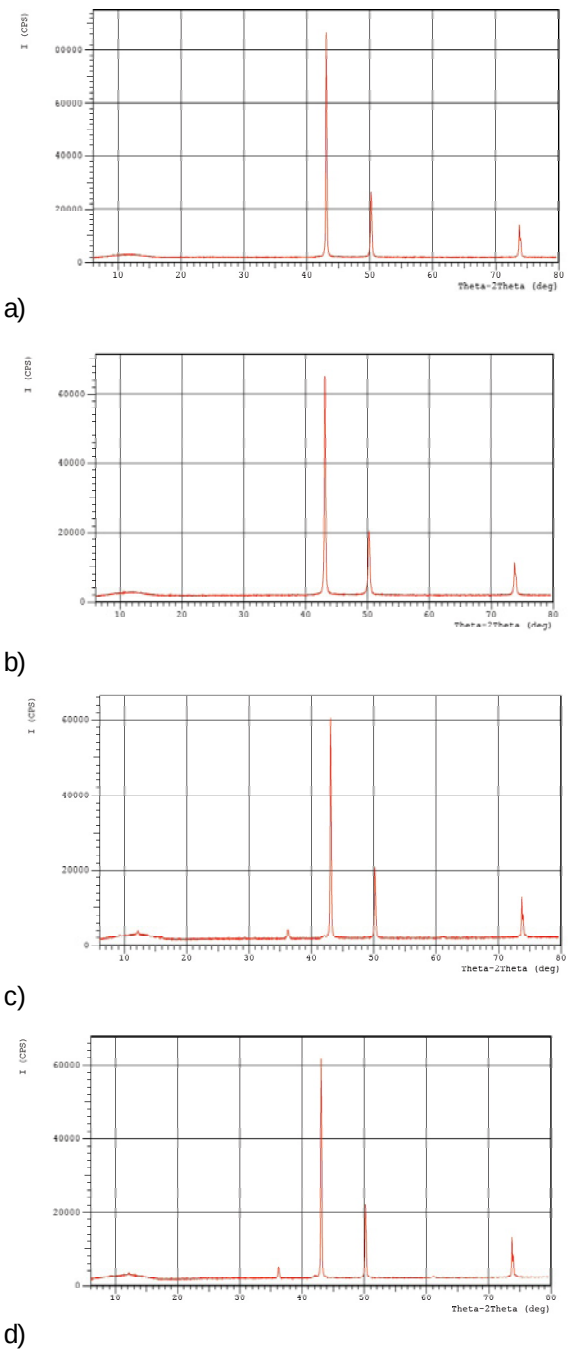

Fig. 6. XRD data: (a) Sample 4, outer surface, (b) Sample 4, inner surface, (c) Sample 1, outer surface, and (d) Sample 3, outer surface.

It is interesting to compare the results of the nanoindentation tests with the data reported by Pavithra et al. [13]. Comparing the data on copper hardness, one can conclude that the results obtained for the film studied are almost twice higher than those reported for the pure annealed copper and are close or even higher than the values stated

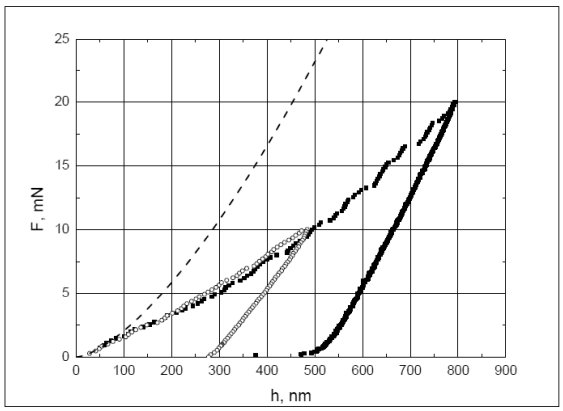

Fig. 7. Loading/unloading curve of the copper film. The Hertz curve is shown as a dashed line.

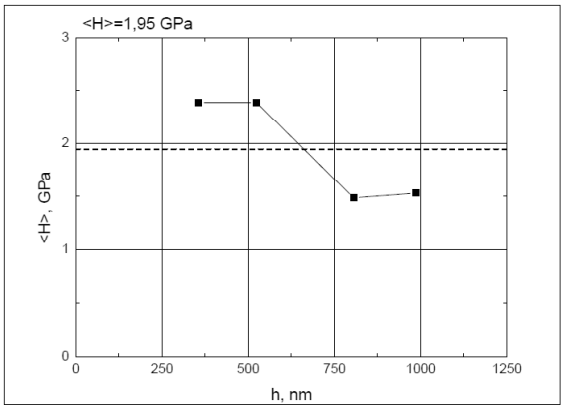

Fig. 9. The dependence of the average hardness values on the indentation depth.

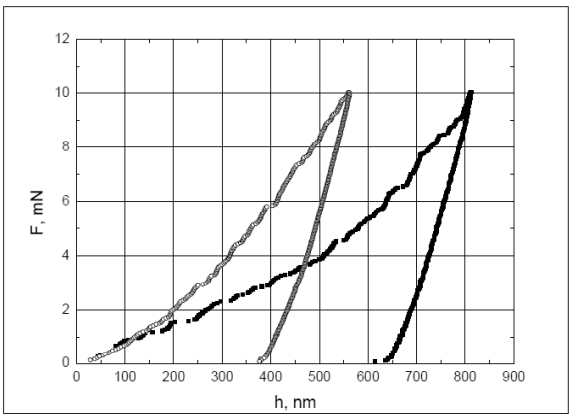

Fig. 8. Nanoindentation data – loading/unloading curve for the copper film at highest and lowest hardness point, loadings < 10 mN.

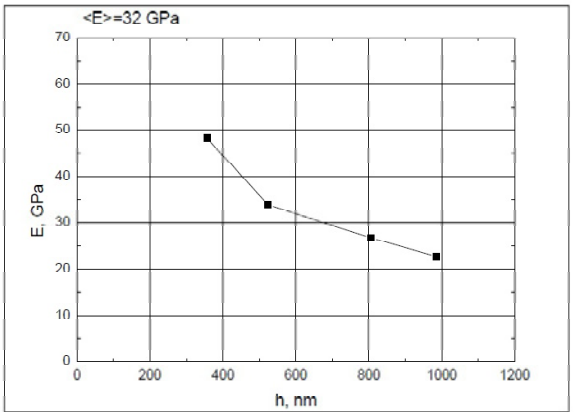

Fig. 9. The dependence of the average Young's modulus values on the indentation depth.

for copper-graphene composite. On the other hand, the values of the elastic modulus for the sample studied are lower than for pure copper.

5. CONCLUSIONS

The task of the current work was the optimization of the electrodeposition approach for the production of nanotwinned copper films with enhanced hardness. The version of the direct current approach with the film growth rate of 340 μm/hour was developed; the manufactured films are characterized by good surface quality. EBSD data indicate nanotwinned structure of the film. Characterization of the films by SEM, XRD, and nonindentation reveals the nanosized crystallites with the typical dimensions of 110-180 nm as a base of the growing films and proves the increase in the material hardness that is twice higher than that for pure annealed copper.

ACKNOWLEDGEMENTS

This work was supported, in part (for VGK and OYuK), by the Ministry of Education and Science of Russian Federation (Zadanie № 9.1964.2014/K), in part (for NNN and IYuA), by the St. Petersburg State University (research grant 6.37.671.2013), and in part (for AVO and ASG) Russian Science Foundation under the grant 14-22-00018.

REFERENCES

[1] Y. Morris Wang, Frederic Sansoz, Thomas LaGrange, Ryan T. Ott, Jaime Marian, Troy W. Barbee Jr and Alex V. Hamza // *Nature Materials* **12** (2013) 697.

[2] T. A. Furnish and A. M. Hodge // Appl. Mater. **2** (2014) 046112-1.

[3] Lei Lu, Yongfeng Shen, Xianhua Chen, Lihua Qian and K. Lu // *Science* **304** (2004) 422.
[4] I.A. Ovidko // *Science* **295** (2002) 2386.
[5] L. Lu, X. Chen, X. Huang and K. Lu // *Science* **323** (2009) 607.
[6] Z.S. You, L. Lu and K. Lu // *Scripta Materialia* **62** (2010) 415.
[7] Z.S. You, L. Lu and K. Lu // *Acta Materialia* **59** (2011) 6927**.**
[8] Zesheng You, Xiaoyan Li, Liangjin Gui, Qiuhong Lu, Ting Zhu, Huajian Gao and Lei Lu // *Acta Materialia* **61** (2013) 217.
[9] In-Chul Choi, Yong-Jae Kim, Y. Morris Wang, Upadrasta Ramamurty and Jae-il Jang // *Acta Materialia* **61** (2013) 7313**.**
[10] Yu. I. Golovin, V.I. Ivolgin, M.A. Lebedkin and D.A. Sergunin // *FTT* **46(9)** (2004) 1618.
[11] Yu. I. Golovin // *FTT* **50(12)** (2008) 2113.
[12] A.C. Fischer-Cripps, *Nanoindentation* (N.Y., Springer, 2004).
[13] Chokkakula L. P. Pavithra, Bulusu V. Sarada, Koteswararao V. Rajulapati, Tata N. Rao and G. Sundararajan // *Scientific reports* **4** (2014) 4049.